Effect of viscogens on the kinetic response of a photoperturbed allosteric protein

Waldauer, Steven A ; Stucki-Buchli, Brigitte ; Frey, Lukas ; Hamm, Peter

Abstract: By covalently binding a photoswitchable linker across the binding groove of the PDZ2 domain, a small conformational change can be photo-initiated that mimics the allosteric transition of the protein. The response of its binding groove is investigated with the help of ultrafast pump-probe IR spectroscopy from picoseconds to tens of microseconds. The temperature dependence of that response is compatible with diffusive dynamics on a rugged energy landscape without any prominent energy barrier. Furthermore, the dependence of the kinetics on the concentration of certain viscogens, sucrose, and glycerol, has been investigated. A pronounced viscosity dependence is observed that can be best fit by a power law, i.e., a fractional viscosity dependence. The change of kinetics when comparing sucrose with glycerol as viscogen, however, provides strong evidence that direct interactions of the viscogen molecule with the protein do play a role as well. This conclusion is supported by accompanying molecular dynamics simulations.

DOI: https://doi.org/10.1063/1.4897975

AIP | The Journal of Chemical Physics

Effect of viscogens on the kinetic response of a photoperturbed allosteric protein

Steven A. Waldauer, Brigitte Stucki-Buchli, Lukas Frey, and Peter Hamm

Citation: The Journal of Chemical Physics **141**, 22D514 (2014); doi: 10.1063/1.4897975
View online: http://dx.doi.org/10.1063/1.4897975
View Table of Contents: http://scitation.aip.org/content/aip/journal/jcp/141/22?ver=pdfcov
Published by the AIP Publishing

Effect of viscogens on the kinetic response of a photoperturbed allosteric protein

Steven A. Waldauer, Brigitte Stucki-Buchli, Lukas Frey, and Peter Hamm[a)]
Department of Chemistry, University of Zurich, Winterthurerstr. 190, CH-8057 Zürich, Switzerland

(Received 6 August 2014; accepted 30 September 2014; published online 17 October 2014)

By covalently binding a photoswitchable linker across the binding groove of the PDZ2 domain, a small conformational change can be photo-initiated that mimics the allosteric transition of the protein. The response of its binding groove is investigated with the help of ultrafast pump-probe IR spectroscopy from picoseconds to tens of microseconds. The temperature dependence of that response is compatible with diffusive dynamics on a rugged energy landscape without any prominent energy barrier. Furthermore, the dependence of the kinetics on the concentration of certain viscogens, sucrose, and glycerol, has been investigated. A pronounced viscosity dependence is observed that can be best fit by a power law, i.e., a fractional viscosity dependence. The change of kinetics when comparing sucrose with glycerol as viscogen, however, provides strong evidence that direct interactions of the viscogen molecule with the protein do play a role as well. This conclusion is supported by accompanying molecular dynamics simulations. © *2014 AIP Publishing LLC*. [http://dx.doi.org/10.1063/1.4897975]

I. INTRODUCTION

The role of solvent friction in protein dynamics and kinetics is an active topic of investigation. Does friction moderate or enable important properties such as allostery or protein function, and if so, by what mechanism? Diffusion models and Kramers theory can provide a basic framework to relate kinetics to solvent viscosity,[1] and systems that deviate from these relations yield important insights. For biomolecular processes, these viscosity relations can have important physiological consequences. For example, the viscosity inside the cellular cytoplasm can differ by greater than ten fold, varying across the type of cell (and species), its life stage, and locally within the cell or organelle.[2] Other studies on this topic have measured the viscosity dependence of small ligand dissociation[3,4] or the folding rates of peptides or of entire proteins.[5–14] Viscosity has an obvious important role in diffusive processes within the cell, but may also have an additional important role in regulating reaction rates and metabolism.

Previously, we presented work on a small protein binding domain, PDZ2, covalently bound with an azobenzene-derived photoswitchable cross-linker.[15] This system is particularly advantageous to study conformational transition kinetics in that most naturally occurring photo-triggerable systems have been limited to a small subset of proteins containing photo-dissociative ligands or isomerizable dyes. In this system, the photoswitch was bound across the binding groove such that photo-isomerization of the linker would mimic ligand binding and an allosteric conformational transition (see Fig. 1). The opening of the binding groove and the overall protein response were observed via UV-pump IR-probe spectroscopy from picoseconds after photo-isomerization out to tens of microseconds. The relaxation kinetics of the binding groove, as monitored by a vibrational mode localized on the photoswitch, were highly nonexponential and when fit to a stretched exponential function were determined to have $\beta \approx 0.5$, a characteristic time constant $\approx$10 ns, and ended within about 100 ns. The response of the protein as a whole, on the other hand, was much more complex, comprising both the nonexponential response of the binding groove and an additional slower response on the microsecond timescale without fully reaching equilibrium within the measurement time window of 40 μs. We speculated that this slower response is related to structural changes in the termini as well as loop regions.

The system was further investigated through non-equilibrium molecular dynamics (MD) simulations where individual trajectories also showed nonexponential kinetics for the opening of the binding groove. The conformational change thus was concluded to be homogeneous, indicating that each molecule evolves on a complex rough energy landscape without any dominant energy barrier. Nonexponential kinetics are theorized to be common for solvent slaved processes,[16] and solvent interactions may be a dominant cause of roughness in the energy landscape and the resulting nonexponential kinetics of the protein response.

An alternative way to view this process is through an anomalous diffusion perspective. In this case the Smoluchowski equation, which describes diffusion, is extended to a fractional Fokker–Plank equation, resulting in non-Markovian dynamics.[17–19] Similar nonexponential kinetics were reported by the Xie group by single molecule studies of protein conformational dynamics, and were explained in part through anomalous subdiffusion.[20] To date, there have been very few further investigations of these phenomena and their relation with solvent viscosity, especially its influence on anomalous diffusion.

[a)]Author to whom correspondence should be addressed. Electronic mail: peter.hamm@chem.uzh.ch

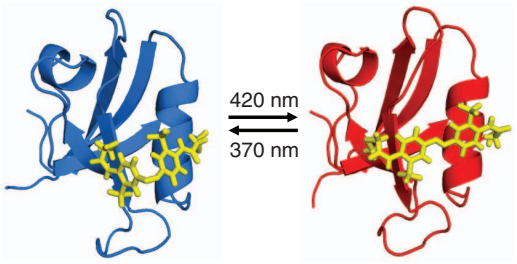

FIG. 1. Nuclear magnetic resonance (NMR) structures of the photoswitch cross linked PDZ2 domain in the *cis* (blue, PDB ID: 2M10) and *trans* (red, PDB ID: 2M0Z) conformations.[15]

In this work, we further investigate the same PDZ2 system described previously and the role of temperature and viscosity. In particular, we will address the question whether the effect of viscogens is solely due to the change of solvent viscosity, or whether direct interactions exist that affect the kinetics as well.

II. METHODS

A. Sample preparation

The double mutated PDZ2 domain, S21C E76C, was expressed from *Escherichia coli*, and the photoswitchable linker 3,3′-bis(sulfonato)-4,4′-bis(chloroacetamido) azobenzene (BSBCA) was covalently attached to two mutation substituted cysteines according to the protocol first described by the Woolley group[21] and detailed in Ref. 15. All experiments were performed in 50 mM borate buffer (pD 9.0) and 150 mM NaCl in D_2O.

Temperature-dependent circular dichroism (CD) spectra were measured on a Jasco J-810 spectroplarimeter. Measurements were taken either at 2 μM in a 1 cm pathlength cuvette and temperature controlled through a peltier or at 20 μM in 0.5 mm pathlength water cooled cuvette and temperature controlled via a closed loop thermal bath/circulator. The melting point, stability, and additional CD analysis were conducted according to standard methods listed in Refs. 22 and 23.

Solution viscosity was controlled through the addition of sucrose or glycerol. Viscosities were estimated through empirical formulas for aqueous sucrose[24] or glycerol[25] solutions determined by weight fraction, and measured directly with a viscometer (Brookfield DV–I+) at 21 °C. Measured viscosities were higher than the empirical values, as expected since the viscosity of D_2O is higher than that of water (see the supplementary material[65]). For time-resolved IR measurements in order to H-D exchange all the accessible hydrogens, sucrose was twice dissolved in excess D_2O and then recrystallized either in a rotivap or lyophilizer before use in any experiment. Fully deuterated glycerol (d-8) was purchased through C/D/N Isotopes Inc. (Pointe-Claire, Canada).

B. Transient IR spectroscopy

The transient IR spectrometer was comprised of two electronically synchronized 1-kHz Ti:sapphire oscillator/regenerative amplifier femtosecond laser systems (Spectra Physics), and described in detail in Ref. 26. The instrument is capable of producing pump-probe delays up to 42 μs with a time resolution of ≈10 ps. The pump pulses used to initiate the *cis*-to-*trans* isomerization of the photoswitch were set to 420 nm, focused to about 100 μm in the sample cell, with energy 3 μJ and stretched to 1 ps. IR probe pulses were provided by an optical parametric amplifier[27] (100 fs, centered near 1450 cm^{-1}) coupled to the second laser system. Detection was performed by a double array 64 element MCT detector.

Prior to every pump-probe pulse pair, the photoswitch conformational state of the sample was fully set in the *cis* conformation through the illumination with a 150 mW continuous wave (cw) diode laser at 370 nm (CrystaLaser). To accomplish this concurrent with measurements, the sample was circulated and reset using two different techniques. The first, described in detail in Ref. 28 and used in our previous PDZ2 studies,[15] employs a closed-cycle flow system. The cw beam illuminates a small volume reservoir that precedes the actual measurement cell, which consisted of two CaF_2 windows separated by 50 μm and a 1 mm wide measurement channel. The second method, necessary for higher solvent viscosity measurements, employed a rotating sample-cell. In this method, the pump/probe beams are focused ≈5–10 mm from the center of a sealed CaF_2 50 μm optical path length cell, and the cw beam illuminates a 2–3 mm diameter spot along the circle traced by and immediately following the overlapping pump and probe beams in the rotating (≈240 rpm) cell. Besides allowing virtually unlimited viscosity, this method also greatly reduced sample volumes, from >450 μl to ≈40 μl/measurement. To reduce sample degradation and surface deposition of the sample onto the cell windows, pulses were stretched to ≈10–100 ps/pulse, by either misaligning or fully removing the compressor stage of the regenerative amplifier.

All of the temperature controlled measurements were taken using a slightly modified closed-cycle flow system, based on the method described above. In these measurements, both the sample cell and the fluid reservoir were temperature controlled, measured at the sample-cell, by a closed-cycle thermal chiller. The cuvette used for the fluid reservoir was a quartz Constant Temperature Cell water-cooled cuvette, model number 62/Q/10 (Starna, Hainult UK).

C. Molecular dynamics simulations

The MD protocol is the same as in Ref. 15. In brief, simulations were performed with the Gromacs program package[29] and the Gromacs implementation of the Charmm27 force field,[30,31] with a timestep of 2 fs, saving time 500 fs, all bonds constrained, NPT ensemble at 300 K and 1 bar, with time constants of 0.2 ps and 0.5 ps, respectively, for the thermostat and the barostat. Lennard-Jones interactions were treated with a cut-off of 1.0 nm (switched to zero at 0.9 nm), and the long range electrostatic forces were approximated by the Particle-Mesh-Ewald approximation. The photoswitch was parameterized as in Ref. 32. To force the photoswitch to be either in the *cis* or the *trans*-configuration, the double minimum potential for the central C–N=N–C dihedral angle was replaced by a single minimum potential,[33–35] and the force constant

increased by a factor 3 such that the potential around the minimum agrees reasonably well with that of the original double minimum potential.

After solvation with 5355 TIP3P water molecules and one Cl^- counter ion to neutralize the simulation box, proper minimization and equilibration of the molecule for 1.1 μs, an ensemble of 300 000 *cis*-starting structures was generated from a subsequent 3 μs *cis*-equilibrium simulation, separated 10 ps each. From these *cis*-starting structures, non-equilibrium MD runs were initiated by instantaneously switching the potential of the central C–N=N–C dihedral angle into *trans*. Simulation times were varied such that the number of samples in each time-bin on a logarithmic time-axis were roughly the same. That is, for the original data with water mass 18 (see black line in Fig. 8 below), 150 000 trajectories were run for 4 ps, 75 000 trajectories for 8 ps, and so on, up to 73 trajectories for 8 ns. In addition, 120 trajectories for [a] full 100 ns were collected. Here, we varied the water mass from *m*/100 to 100*m* in order to mimic a viscosity change of the solvent. A similar sampling scheme was used with a reduced amount of sampling, i.e., 37500 trajectories with 1 ps, 18750 trajectories with 2 ps, and so on, up to 146 trajectories with 250 ps plus 73 trajectories with 10 ns. In the case of water mass 100*m*, 73 additional trajectories with 100 ns were collected. For the simulations with water masses *m*/100 and *m*/10, the timestep was reduced to 0.2 fs and 0.63 fs, respectively.

III. TRANSIENT IR SPECTROSCOPY

The kinetic response of the protein binding groove was measured through pump-probe IR spectroscopy. To that end, the initial state of the photoswitch was set to the *cis* state and at time zero, a UV pump pulse photoisomerized the switch to the *trans*-state. Difference spectra between switched and non-switched conformations were recorded at logarithmic time delays ranging from −10 ps to 25 μs by an IR broadband pulse centered at about 1450 cm^{-1}. Part of this spectral window, shown in Fig. 2, contains a distinct mode at about 1490 cm^{-1} resulting from two amide groups integral to the attached photoswitch, i.e., essentially its N-D bending mode. A small shift and change in intensity of this band is visible in the transient difference spectra as a peak slightly below 1490 cm^{-1} and a valley at about 1480 cm^{-1}. This signal is an excellent reporter on the conformation of the binding groove because it is a local mode directly on the photoswitch. The band is visible both when the photoswitch is attached to the protein and for measurements of the photoswitch alone, with the kinetics being slowed down significantly in the former case (see blue circles in Fig. 3 of Ref. 15). Consequently, the protein response is rate-limiting for the kinetics of that band.

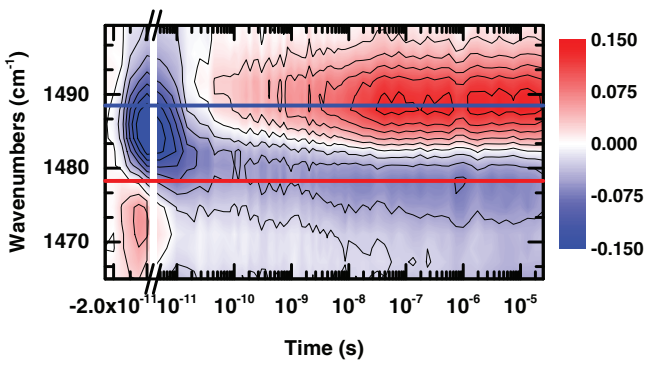

FIG. 2. An illustrative example of time-resolved difference-spectra, taken at 21°C and 0% w/w sucrose, showing growth of a peak at 1488 cm^{-1} (blue line) and valley at 1478 cm^{-1} (red line).

Time traces taken from the difference peak at 1488 cm^{-1} and valley at 1478 cm^{-1} show essentially identical kinetics. In order to entirely compensate for any broadband offsets, such as those resulting from thermal lensing, the kinetics of the groove relaxation are taken from the difference between these two signals. Visible in the time traces are two distinct phases (see Fig. 3). The first phase, extending to ≈100 ps is a strong, structured signal spanning the entire spectral range. This phase is a direct result of the absorption of the 420 nm pulse by the photoswitch azobenzene moiety and its subsequent ultrafast isomerization. This results in the deposition of a large amount of energy into the vibrational degrees of freedom of the linker and the protein, which appears as heat.[36] This phase becomes much less prominent when the pump pulse becomes stretched, and is almost negligible with 100 ps pulses.

The second phase, observable after the dissipation of the heat signal, is indicative of the opening of the binding groove. The relaxation is highly nonexponential and extends to about 100 ns. It is possible to fit the two phases, heat signal and opening of the binging groove, with a sum of a single exponential and a stretched exponential function, respectively:

$$q(t) = a_0 + a_1 e^{-(t/\tau_1)} + a_2 e^{-(t/\tau_2)^\beta}. \quad (1)$$

For a stretched exponential function, the average time of the process is given by[37]

$$\langle \tau \rangle \equiv \int_0^\infty t \cdot e^{-(t/\tau)^\beta} dt = \frac{\tau}{\beta} \Gamma\left(\frac{1}{\beta}\right). \quad (2)$$

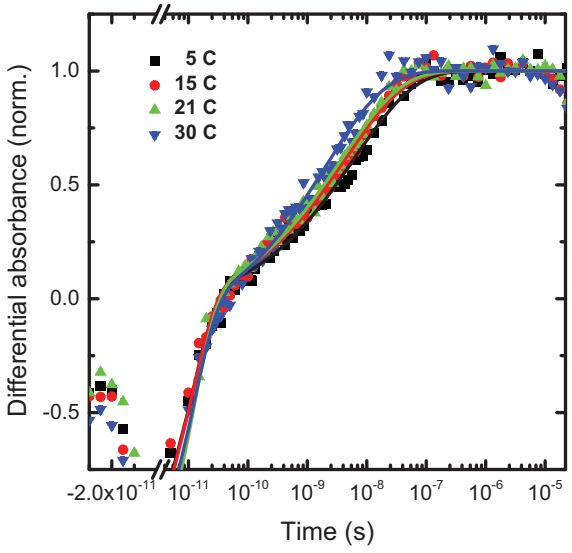

FIG. 3. Normalized differential absorption with temperatures 5°C, 15°C, 21°C, and 30°C and with 0% w/w sucrose. Lines show a global fit to Eq. (1) (see text for details).

A. Temperature dependence

CD spectroscopy revealed melting temperatures of 37 °C for the native PDZ2 domain without photoswitch, 42 °C for the linked PDZ2 domain with the photoswitch in *trans*, and 44 °C for the photoswitch in *cis* (see Fig. S1 in the supplementary material[65]). Hence, over a temperature range of 5–30 °C, one is in a regime where the protein is stably folded in both states of the photoswitch and one can study the temperature dependence of the switching kinetics without further complications due to partial unfolding of the protein. Figure 3 shows the result with a measurable temperature variation. Global fitting of the data turned out to be more stable. To that end, all the curves were fitted simultaneously with both the time constant for the heat signal ($\tau_1 = 12.5$ ps) and the stretching factor ($\beta = 0.46$) forced to be the same for all temperatures, while τ_2 as well as the amplitudes were allowed to vary independently. The reduced χ^2 values using this methodology were within 0.5% of fits when both β and τ_2 were allowed to float.

The resulting averaged times $\langle\tau_2\rangle$ were combined from β and τ_2 according to Eq. (2) and are summarized in Fig. 4 in an Arrhenius plot. When analyzing these data on the level of an Arrhenius equation,

$$k = k_0 e^{-E^{\ddagger}/k_B T}, \tag{3}$$

one estimates an activation barrier of $E^{\ddagger} = 7.3$ kcal/mol. We note, however, that the solvent viscosity changes by a factor of two in the considered temperature range; for D_2O it is 2.0 cP at 5 °C and 0.9 cP at 30 °C (see the supplementary material[65]). If a linear viscosity dependence of the rate is assumed, as commonly done (see discussion below), normalizing by viscosity,

$$k' = k\frac{\eta}{\eta_0}, \tag{4}$$

cancels out most of the temperature dependence of the rate (Fig. 4, red triangles). In that case, the fit to Eq. (3) reveals a correspondingly smaller value $E^{\ddagger} = 2.2$ kcal/mol.

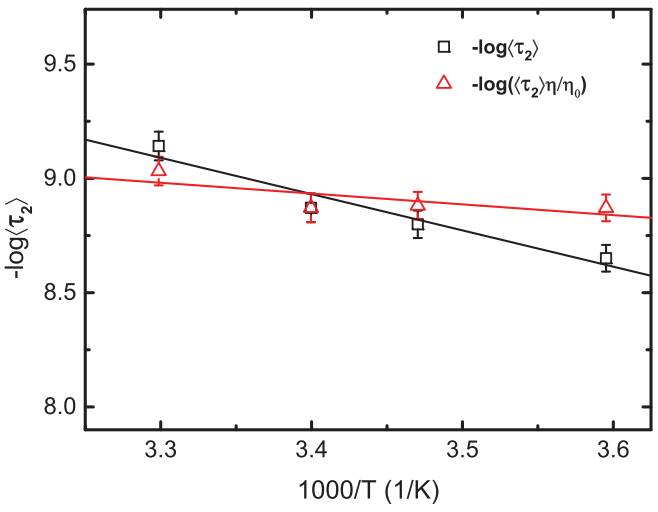

FIG. 4. Arrhenius plot of the rate $1/\langle\tau_2\rangle$ of the binding groove relaxation (black) and the solvent viscosity corrected rates $1/\langle\tau_2\rangle \cdot \eta/\eta_0$ (red).

Alternatively, one may invoke a super-Arrhenius temperature dependence

$$D = D_0 e^{-(\epsilon/k_B T)^2}, \tag{5}$$

which has been used to describe diffusion on a rugged potential energy surface, and in which case ϵ is a measure of its ruggedness.[38] While within the narrow temperature range of Fig. 4 we cannot distinguish an Arrhenius from a super-Arrhenius temperature dependence, if we assume the latter, we estimate for the ruggedness $\epsilon = 1$ kcal/mol, or $\epsilon = 0.6$ kcal/mol after normalizing by viscosity, and, i.e., a value in the order of $2\,k_BT$. It is worthwhile noting that a similar roughness has been reported recently for the downhill folding of a β-sheet with $\epsilon = 2.4$ kcal/mol.[39]

In our previous PDZ2 study,[15] we provided evidence from MD simulations that the nonexponential relaxation of the binding groove is of homogeneous origin, in that individual simulated trajectories displayed essentially identical kinetics to that of the averaged ensemble (apart from statistical fluctuations).[40] In particular, individual trajectories did not show any two-state behavior, but propagated continuously. We therefore concluded that the reaction does not proceed via a single dominant barrier, but rather has to be viewed as downhill diffusion on a rugged free-energy landscape. The experimentally observed temperature dependence is not really conclusive in this regard, as both scenarios, barrier hopping Eq. (3) *versus* diffusion Eq. (5), would reveal reasonable values for the energy barrier or ruggedness, respectively. We nevertheless reason that the experimental result does not contradict the conclusion drawn from the MD simulation of Ref. 15.

B. Viscosity dependence

The relaxation kinetics were then measured at different solvent viscosities by varying the sucrose concentration from 0 to 50% w/w. This produces a range of solvent viscosities from 1.2 to 25.0 cP. Figure 5 shows time traces of the binding groove relaxation kinetics at six different viscosities. There is no observable correlation between the initial heat signal and viscosity. There is, however, a visible change in the nonexponential phase, with a definite decrease in the relaxation rate with increasing viscosity.

The results are compiled in Fig. 6(a), which plots the average time $\langle\tau_2\rangle$ as a function of viscosity. The red line shows a linear fit

$$\langle\tau_2\rangle = \langle\tau_2^{(0)}\rangle + \alpha \cdot \eta, \tag{6}$$

incorporating a non-zero y-intercept of $\langle\tau_2^{(0)}\rangle \approx 6$ ns at zero solvent viscosity, which commonly would be interpreted as "internal friction" (see discussion).[5,6,10,11] Alternatively, a "fractional" viscosity dependence has been imposed, described by a power law:[8]

$$\langle\tau_2\rangle \propto \eta^{\gamma}, \tag{7}$$

which reveals $\gamma = 0.69$ (blue line). While the error bars are not quite small enough to firmly exclude the linear fit, the power-law fit does provide a significantly better representation of the data.

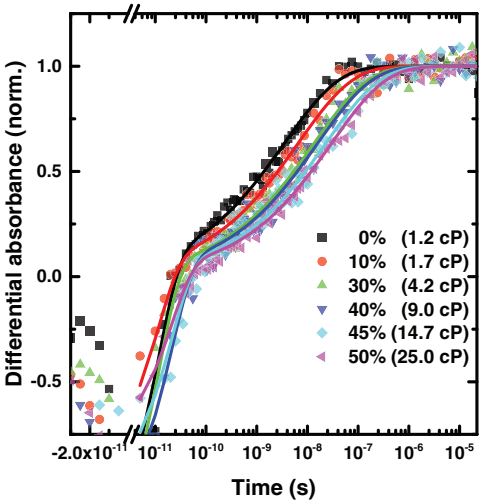

FIG. 5. Normalized differential absorption with sucrose concentrations 0% w/w, 10% w/w, 30% w/w, 40% w/w, 45% w/w, and 50% w/w, resulting in solvent viscosities of 1.2 cP, 2.7 cP, 4.2 cP, 9.0 cP, 14.7 cP, and 25.0 cP, respectively. All measurements were performed at 21°C. Lines show a global fit to Eq. (1) (see text for details).

To set the stage, we start with the Stokes-Einstein relation

$$D = k_B T / 6\pi\eta R, \tag{8}$$

which predicts the time it takes for a diffusive process to scale linearly with time. The same linear dependence is obtained from Kramers theory in the diffusive regime for a barrier hopping process,[1] and, more trivially, for the relaxation of a harmonic oscillator in the strongly over-damped regime.[41] Based on that notion, it is reasonable to divide friction into two contributions[5,6,10,11]

$$\xi = \xi_{int} + \xi_{solvent}(\eta) = \xi_{int} + \alpha' \cdot \eta, \tag{9}$$

i.e., internal friction and friction imposed by the solvent, the latter of which scales linearly with viscosity, which is the motivation for the linear fit Eq. (6) (Fig. 6(a), red line). Sources of internal friction could be breaking and reforming of intra-protein hydrogen bonds, backbone and side chain rotations or steric clashes, depending on whether the corresponding degrees of freedom are solvent exposed, e.g., for unfolded chains, or whether they are buried inside the hydrophobic core. In particular the contribution of dihedral rotations to internal friction has been studied in quite some detail recently.[14]

The same behavior has been observed before for various molecular systems. For example, Ref. 5 found exactly these two contributions for the end-to-end fluctuations of an unstructured peptide as a function of chain length and solvent viscosity. There are, however, numerous reports on molecular processes with a nonlinear, fractional viscosity dependence,[12,42–44] which often goes hand-in-hand with non-exponential relaxation kinetics, just like in our present case. Common to many of these processes is their mostly barrierless nature.[43,44] Also the folding of protein secondary structure motifs of small peptides such as α-helix folding, which are known to deviate from two-state behavior, commonly follows stretched exponential kinetics with stretching factors around $\beta = 0.7$–0.8.[34,45] At the same time, the viscosity dependence of such processes has been shown to be fractional with $\gamma = 0.6$.[7] Based on MD simulations, Ref. 10 demonstrated that even very short peptides show a nonzero folding time when viscosity is extrapolated to zero (by varying the water mass) and that the mean passage time for end-to-end distances exhibit a complex interplay of both linear and power-law behavior depending on the solvent viscosity regime, internal friction strength, and polymer size.

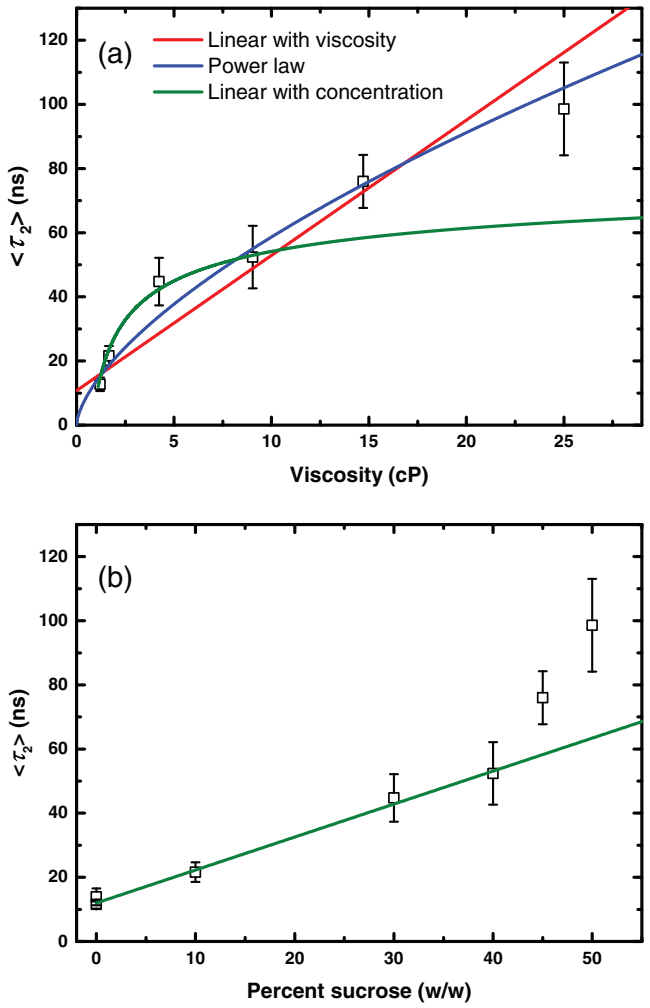

FIG. 6. (a) Comparison of the averaged time $\langle\tau_2\rangle$ of the binding-groove relaxation as a function of viscosity. The red line shows the data fit to a linear viscosity dependence, the blue line to a fractional viscosity dependence. (b) Comparison of the same averaged time $\langle\tau_2\rangle$ as a function of sucrose concentration in % w/w and fit linearly up to 40% w/w sucrose. The green line in Panel (a) shows a transformation of the linear fit in Panel (b), using the nonlinear dependence of the viscosity on viscogen concentration.

C. Viscogen dependence

To further investigate the influence of the particular viscogen molecule, an additional experiment was performed comparing the kinetics of the binding groove relaxation with sucrose and glycerol at the same solvent viscosity, 9.4 cP. To reach that value, a concentration of 40% w/w was needed for sucrose and 54% w/w for glycerol (see Fig. S2 in the supplementary material[65]). The two viscogens differ by almost a factor four in molecular weight (sucrose: MW 342 and

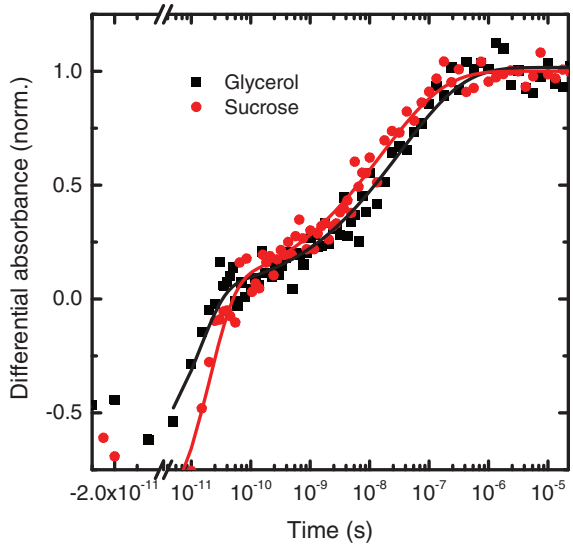

FIG. 7. Normalized differential absorption binding groove relaxation kinetics at ≈9.4 cP solvent viscosity comparing glycerol (black) and sucrose (red) as viscogens. Lines show a global fit to Eq. (1).

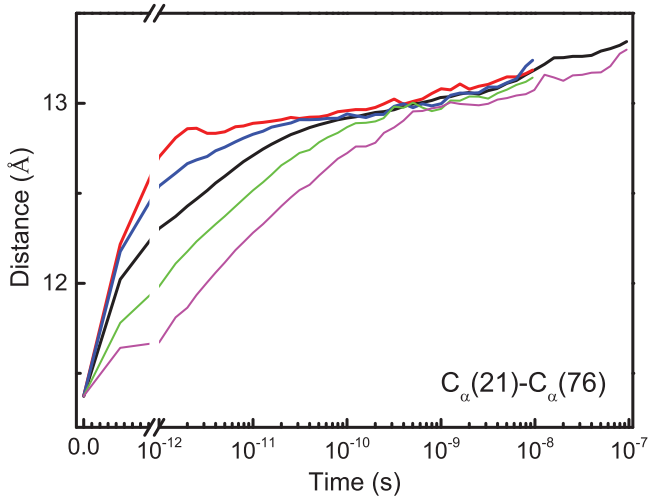

FIG. 8. MD results for the opening of the binding groove, measured via the $C_\alpha(21)$-$C_\alpha(76)$ distance. The black line is for normal water with mass $m = 18$, taken from Ref. 15. Red, blue, green, and magenta lines are for $m/100$, $m/10$, $10m$, and $100m$, respectively.

glycerol: MW 92), but both have been argued to be highly preferably excluded from the protein surface.[46–48]

Nevertheless, Fig. 7 shows that glycerol significantly slows the relaxation kinetics in comparison with sucrose. The effect might appear small on the logarithmic scale of Fig. 7, but is clearly beyond our error bar. To that end, see Fig. S3 in the supplementary material,[65] which shows two measurements under identical conditions taken at two different days separated by months, which demonstrates the degree of reproducibility of these experiments. Fitting the traces in the same manner as described above yields an averaged time of $\langle\tau_2\rangle = 50$ ns for sucrose and $\langle\tau_2\rangle = 105$ ns for glycerol. In agreement with Refs. 4 and 13 we thus conclude that the kinetics of the binding groove relaxation is not exclusively a function of the solvent viscosity, but specific interactions with the particular viscogen molecule seem to play a role as well.

IV. MOLECULAR DYNAMICS SIMULATIONS

To gain a molecular insight into the underlying mechanism, MD simulations have been performed. Computationally, changing the mass of water is a very elegant and clean way to explore the viscosity dependence of the switching process, without changing anything else but the solvent friction.[10,49–51] That is, it can been shown on very general grounds that within the framework of classical mechanics, any thermodynamic property of a system is not dependent on atom masses,[52] only dynamical properties are. In particular, the starting and ending ensembles before and after switching, respectively, ought to be the same.

Fig. 8 plots the kinetics of the $C_\alpha(21)$-$C_\alpha(76)$ distance of the two cysteines onto which the photoswitch is bound, with the mass of the water varied from $m/100$ to $100m$, thereby changing the viscosity of the solvent from $\eta/10$ to 10η (since the viscosity scales as $\eta \propto \sqrt{m}$). We reiterate from Ref. 15 that the binding groove, measured via the $C_\alpha(21)$-$C_\alpha(76)$ distance, opens in a highly non-exponential manner (Fig. 8, black line), covering timescales from 1 ps to beyond 100 ns (which is the limit of our accessible simulation time). We concluded that the $C_\alpha(21)$-$C_\alpha(76)$ distance is essentially what is measured in the experiment via the localized linker mode observed in Fig. 2. That experimental observable evolves on roughly the same timescale as the $C_\alpha(21)$-$C_\alpha(76)$ distance in the MD simulation and in a similar non-exponential fashion (it would be desirable to link the MD simulations more closely to the IR observable, as recently done for comparable protein systems,[53–56] which would be an interesting avenue for a future investigation).

Fig. 8 shows that solvent viscosity affects the dynamics in two different ways. Most prominent is the effect on the fast time window up to ≈100 ps, where increasing solvent viscosity slows down the process. In addition, for very small frictions ($m/100$, red line), the initial jump is underdamped with a small oscillatory contribution on a 2 ps timescale. However, in contrast to what we had concluded in Ref. 15 (where we compared the full simulation with an implicit water simulation), a small water friction affects the dynamics of the binding groove only up to ≈100 ps, whereas afterwards it follows the normal water mass simulation. It is important to note that in the experiment, we cannot observe that early time window, since the time-scale up to ≈100 ps is masked by the heat signal (Fig. 5).

In the time window beyond ≈1 ns, only the highest viscosity simulation at 100 times the mass of normal water (Fig. 8, magenta line) deviates from the normal mass simulation (black line, by block-averaging we verified that this deviation is statistically significant). In that case, the viscosity is 10 times larger than that of normal water, which is the viscosity range we do reach in our experiments at ≈40–45% w/w sucrose concentration (Figs. 5 and 6(a)).

Taking these observations together, friction indeed consists of a part that originates from the solvent and one that originates from the protein. However, for the process that dominates the faster time window up to ≈100 ps, both contributions do not add up in the sense of Eq. (9). If they

would, water friction would affect the dynamics over the entire timespan for all viscosities, which is not what is observed. On the other hand, the effect observed only for the highest viscosity at water mass 100m in the time window $\gtrsim$1 ns (Fig. 8, magenta line) might probably be described on that level. However, the protein contribution ξ_{int} is larger in a relative sense in the MD simulation, as we observe a significant slow-down only at 10 times the pure water viscosity. On the contrary, the effect is already dominant at 3 times the pure water viscosity in the experimental results (reached at ≈30% w/w sucrose concentration, see Figs. 5 and 6(a)).

V. MERGING EXPERIMENTAL AND MD RESULTS

How do these partially conflicting observations go together? We think that the clue lies in the non-exponential response, i.e., in the fact that the overall response consists of several processes with a range of timescales. The argument starts from the observation that a overdamped diffusive process on a 1D harmonic free energy surface relaxes, of course, exponentially to its minimum after a perturbation.[41] As pointed out in Ref. 57, a free energy surface without any dominant barrier, *per se*, does not yet reveal a non-exponential response. It has therefore often been stated that a non-exponential response is related to diffusion in multi-dimensions.[58,59] That is to say that the coordinate along which we perturb and/or observe the system (i.e., the width of the binding groove in our concrete example) is not a "good" reaction coordinate, in the sense that a free energy projected onto that coordinate cannot describe the dynamics of the system with the help of a memory-free Langevin or diffusion equation. In the Appendix, we present a simple harmonic model with additional hidden coordinates. As they relax after a perturbation, their projection onto the observation coordinate will all contribute, leading to a stretched-exponential response that consists of a sum of exponential responses for each of the relaxing coordinates (Eq. (A7)). In that framework, the MD results from Fig. 8 are interpreted in terms of a faster set of coordinates, which in essence describes water relaxation, and the slower set of coordinates for the relaxation of protein intramolecular degrees of freedom. The latter is affected by water viscosity only at the highest viscosity value studied (Fig. 8, magenta line) This scenario, however, leads to the conclusion that the viscogen does affect the kinetics not only through the solvent viscosity, but also indirectly through explicit interactions of viscogen molecules with the protein. The two-fold difference in the kinetics when using glycerol or sucrose as viscogen at concentrations that lead to the same solvent viscosity (Fig. 7) provide strong evidence for that conclusion.

One finds conflicting views on the effect of these viscogens in literature. For example, it has been argued that both glycerol and sucrose are highly preferably excluded from the protein surface,[46–48] that gylcerol preferentially hydrates proteins,[60] and that these viscogens affects ligand dynamics in myoglobin only via the solvent viscosity, but not in a viscogen-specific way.[3] On the other hand, these viscogens also act as osmolytes and/or crowders, which often work through direct interactions with the protein, e.g., by attenuating the H-bond strength between polar protein residues and water,[61] or by interaction to the protein backbone with different strength.[62] However, one has to keep in mind that most of these works address protein folding, whereas here the molecule stays in a folded state throughout the conformation transition. But also for example for the O_2 escape from respiratory proteins, an inverse correlation between the viscogen molecular weight and its effectiveness at slowing dynamics has been found.[4,13]

In a sense, solvent viscosity might be considered just a measure of the concentration of viscogen molecules, and indeed, plotting the averaged time $\langle\tau_2\rangle$ against sucrose concentration rather than solvent viscosity reveals a linear dependence up to 40% w/w sucrose concentration (Fig. 6(b)). According to the law of mass action, the amount of viscogen molecules directly binding to the protein should scale linearly with concentration (unless saturation is reached). In that case, the power-law dependence of Fig. 6(a) (blue line) would be a trivial result from just the highly nonlinear dependence of the viscosity on the viscogen concentration (see Fig. S2 and Eq. (S1) in the supplementary material[65]).[24,25] In fact, when inverting that nonlinear concentration-viscosity dependence and transforming the linear fit of Fig. 6(b) into the coordinates of Fig. 6(a), a fit of the data even better than the power-law fit is obtained up to a viscosity of 10 cP (Fig. 6(a), green line). That viscosity corresponds to 40% w/w sucrose, or 1.5 M. Beyond this value, other effects take over which probably are related to the fact that the solvent can no longer be considered a dilute solution of sucrose in water.

VI. CONCLUSION

Our results raise questions about the current view on preferential hydration and exclusion of co-solvents. Based on thermodynamic arguments, it has been argued that certain viscogens, such as in particular sucrose and glycerol, may be entirely excluded from the protein hydration shell.[63,64] This conclusion has found support from experimental techniques such as high precision densimetry,[46] neutron scattering experiments,[47] or the vibrational lifetime of a surface exposed protein labels.[48]

While the question whether or not specific interactions of the viscogen molecule with the protein play a role might depend on the particular process studied, in our case they clearly do. In this regard it might be worth mentioning that the structural change initiated by the photoswitch is very small with an RMSD of 0.8–0.9 Å according to NMR structure analysis.[15] In particular, the protein stays stably folded in both states of the photoswitch. In contrast, during protein folding, for which most viscosity dependent studies have been performed,[5–12] the molecule goes through many stages with many shapes, in which case friction deduced from these experiments is an averaged property. As such, our photoswitchable allosteric protein constitutes a very well defined system that allows one to cleanly dissect direct interactions of the viscogen molecules from indirect viscosity effects.[65]

ACKNOWLEDGMENTS

We thank Ben Schuler and his group, in particular Andrea Soranno, for tremendous help with the viscosity

measurements, and Gerhard Stock and Amedeo Caflisch for important discussions. The work has primarily been supported by an ERC advanced investigator grant (DYNALLO) and in part by the Swiss National Science foundation through the NCCR MUST.

APPENDIX: A MODEL FOR THE NON-EXPONENTIAL RESPONSE

In the following, we construct a model to explain the non-exponential response, which we believe contains the correct physics despite its simplicity. To that end, we consider a multidimensional harmonic free energy surface along coordinates $\{q_i\}$:

$$F(\mathbf{q}) = \sum_{i=0}^{n} \omega_i^2 q_i^2 + \sum_{i=1}^{n} \chi_{0,i} q_0 q_i, \tag{A1}$$

where q_0 is the "observation coordinate," and all other q_i with $i = 1 \ldots n$ are hidden coordinates. The frequencies ω_i are measures of the curvatures of the potential along q_i, and the bilinear terms $\chi_{0,i}$ couple the observation coordinate to the hidden coordinates (without loss of generality, we can discard couplings χ_{ij} of hidden coordinates among each other). In our concrete case, the observation coordinate q_0 is both the coordinate along which we perturb the system (i.e., the width of the binding groove), and the "spectroscopic coordinate" whose change we observe (since the band in Fig. 2 is localized on the photoswitch).

In analogy to a normal mode transformation, one can find a unitary transformation C_{ij}:

$$q_i = \sum_{ij} C_{ij} q'_j \tag{A2}$$

such that the couplings disappear in the new set of coordinates $\{q'_i\}$:

$$F(\mathbf{q}') = \sum_{i=0}^{n} \omega_i'^2 q_i'^2. \tag{A3}$$

As we consider a free energy surface rather than a potential energy surface, one should think of these "normal modes" as principle components.

We now mimic a non-equilibrium experiment (in our concrete case due to the photoswitch) by perturbing the system with a linear force A along q_0:

$$F(\mathbf{q}') = \sum_{i=0}^{n} \omega_i'^2 q_i'^2 + q_0 A = \sum_{i=0}^{n} \omega_i'^2 q_i'^2 + C_{0,i} A q'_i. \tag{A4}$$

One can easily show that the minimum of the displaced free energy surface Eq. (A4) is offset by

$$q_i'^{(0)} = \frac{C_{i,0} A}{2\omega_i'^2} \tag{A5}$$

relative to the unperturbed free energy surface Eq. (A3). Provided that the couplings $\chi_{0,i}$ do not vanish, the matrix C_{ij} will not be the identity matrix, and the system is displaced with respect to all coordinates q'_i.

The reason why we had constructed normal modes is because the multidimensional diffusion equation decouples in them. Furthermore, since it is a harmonic free energy surface, we can solve the diffusion equation analytically and obtain for the strongly overdamped case[41]

$$\langle q'_i \rangle(t) = \langle q_i'^{(0)} \rangle e^{-\frac{\omega_i'^2}{\xi'_i} t} = \frac{C_{i,0} A}{2\omega_i'^2} e^{-\frac{\omega_i'^2}{\xi'_i} t}, \tag{A6}$$

where $\langle \ldots \rangle$ symbolized the mean of a distribution, and ξ'_i is the friction along coordinate i'. For each relaxing coordinate, we will see only the projection onto q_0, since q_0 is the spectroscopic coordinate, so overall we will observe

$$\langle q_0 \rangle(t) = \sum_i \frac{C_{i,0}^2 A}{2\omega_i'^2} e^{-\frac{\omega_i'^2}{\xi'_i} t}, \tag{A7}$$

i.e., a multi-dimensional decay with all positive prefactors. Mathematically speaking, this is, of course, *not* a stretched-exponential function. However, if we write a stretched exponential function as a continuous distribution of exponential decays:

$$e^{-(t/\tau)^\beta} = \int_0^\infty \rho(\tau') e^{-t/\tau'} d\tau', \tag{A8}$$

the distribution of time constants $\rho(\tau')$ is in fact positive for all τ'.[37] When fitting an experimentally observed relaxation process as a stretched exponential function, the resulting stretching factor β is a measure of the width of the distribution $g(\tau')$.

[1] P. Hänggi, P. Talkner, and M. Borkovec, Rev. Mod. Phys. **62**, 251 (1990).
[2] A. D. Keith and W. Snipers, Science **183**, 666 (1974).
[3] D. Beece, L. Eisenstein, H. Frauenfelder, D. Good, M. C. Marden, L. Reinisch, A. H. Reynolds, L. B. Sorensen, and K. T. Yue, Biochemistry **19**, 5147 (1980).
[4] S. Yedgar, C. Tétreau, B. Gavish, and D. Lavalette, Biophys. J. **68**, 665 (1995).
[5] E. Haas, E. Katchalski-Katzir, and I. Z. Steinberg, Biopolymers **17**, 11 (1978).
[6] A. C. Ansari, C. M. Jones, E. R. Henry, J. Hofrichter, and W. A. Eaton, Science **256**, 1796 (1992).
[7] G. S. Jas, W. A. Eaton, and J. Hofrichter, J. Phys. Chem. B **105**, 261 (2001).
[8] R. R. Cheng, T. Uzawa, K. W. Plaxco, and D. E. Makarov, J. Phys. Chem. B **113**, 14026 (2009).
[9] S. J. Hagen, Curr. Protein Pept. Sci. **11**, 385 (2010).
[10] J. C. F. Schulz, L. Schmidt, R. B. Best, J. Dzubiella, and R. R. Netz, J. Am. Chem. Soc. **134**, 6273 (2012).
[11] A. Soranno, B. Buchli, D. Nettels, R. R. Cheng, S. Müller-Späth, S. H. Pfeil, A. Hoffmann, E. A. Lipman, D. E. Makarov, and B. Schuler, Proc. Natl. Acad. Sci. U.S.A. **109**, 17800 (2012).
[12] A. Sekhar, P. Vallurupalli, and L. E. Kay, Proc. Natl. Acad. Sci. U.S.A. **109**, 19268 (2012).
[13] A. Sekhar, M. P. Latham, P. Vallurupalli, and L. E. Kay, J. Phys. Chem. B **118**, 4546 (2014).
[14] I. Echeverria, D. E. Makarov, and G. A. Papoian, J. Am. Chem. Soc. **136**, 8708 (2014).
[15] B. Buchli, S. A. Waldauer, R. Walser, M. L. Donten, R. Pfister, N. Blöchliger, S. Steiner, A. Caflisch, O. Zerbe, and P. Hamm, Proc. Natl. Acad. Sci. U.S.A. **110**, 11725 (2013).
[16] P. W. Fenimore, H. Frauenfelder, B. H. McMahon, and F. G. Parak, Proc. Natl. Acad. Sci. U.S.A. **99**, 16047 (2002).
[17] R. Metzler, E. Barkai, and J. Klafter, Phys. Rev. Lett. **82**, 3563 (1999).
[18] W. G. Glöckle and T. F. Nonnenmacher, Biophys. J. **68**, 46 (1995).
[19] G. R. Kneller and K. Hinsen, J. Chem. Phys. **121**, 10278 (2004).
[20] H. Yang and X. S. Xie, J. Chem. Phys. **117**, 10965 (2002).
[21] D. C. Burns, F. Zhang, and G. A. Woolley, Nat. Protoc. **2**, 251 (2007).

[22]A. K. J. Kizhakkedathu, M. Nazeerunnisa, and D. V. Behere, J. Biol. Chem. **277**, 40717 (2002).
[23]S. M. Kelly, T. J. Jess, and N. C. Price, Biochim. Biophys. Acta **1751**, 119 (2005).
[24]M. Mathlouthi, and J. Génotelle, in *Sucrose*, edited by M. Mathlouthi and P. Reiser (Springer, Boston, MA, 1995), pp. 126–154.
[25]B. B. Hasinoff, Arch. Biochem. Biophys. **183**, 176 (1977).
[26]J. Bredenbeck, J. Helbing, and P. Hamm, Rev. Sci. Instrum. **75**, 4462 (2004).
[27]P. Hamm, R. A. Kaindl, and J. Stenger, Opt. Lett. **25**, 1798 (2000).
[28]J. Bredenbeck and P. Hamm, Rev. Sci. Instrum. **74**, 3188 (2003).
[29]D. van der Spoel, E. Lindahl, B. Hess, G. Groenhof, A. E. Mark, and H. J. C. Berendsen, J. Comput. Chem. **26**, 1701 (2005).
[30]A. D. Mackerell, M. Feig, and C. L. Brooks III, J. Comput. Chem. **25**, 1400 (2004).
[31]A. D. Mackerell, D. Bashford, M. Bellott, R. L. Dunbrack, J. D. Evanseck, M. J. Field, S. Fischer, J. Gao, H. Guo, S. Ha *et al.*, J. Phys. Chem. B **102**, 3586 (1998).
[32]S. Spörlein, H. Carstens, H. Satzger, C. Renner, R. Behrendt, L. Moroder, P. Tavan, W. Zinth, and J. Wachtveitl, Proc. Natl. Acad. Sci. U.S.A. **99**, 7998 (2002).
[33]P. H. Nguyen and G. Stock, Chem. Phys. **323**, 36 (2006).
[34]J. A. Ihalainen, B. Paoli, S. Muff, E. H. G. Backus, J. Bredenbeck, G. A. Woolley, A. Caflisch, and P. Hamm, Proc. Natl. Acad. Sci. U.S.A. **105**, 9588 (2008).
[35]S. Buchenberg, V. Knecht, R. Walser, P. Hamm, and G. Stock, "Long-Range Conformational Transition of a Photoswitchable Allosteric Protein: A Molecular Dynamics Simulation Study" J. Phys. Chem. B (submitted).
[36]P. Hamm, S. M. Ohline, and W. Zinth, J. Chem. Phys. **106**, 519 (1997).
[37]F. Alvarez, A. Alegria, and J. Colmenero, Phys. Rev. B **44**, 7306 (1991).
[38]R. Zwanzig, Proc. Natl. Acad. Sci. U.S.A. **85**, 2029 (1988).
[39]Y. Xu, P. Purkayastha, and F. Gai, J. Am. Chem. Soc. **128**, 15836 (2006).
[40]H. Frauenfelder, G. Chen, J. Berendzen, P. W. Fenimore, H. Jansson, B. H. McMahon, I. R. Stroe, J. Swenson, and R. D. Young, Proc. Natl. Acad. Sci. U.S.A. **106**, 5129 (2009).
[41]H. Goldstein, C. P. Poole, and J. L. Safko, *Classical Mechanics* (San Francisco: Addison Wesley, 2002).
[42]S. P. Velsko, D. H. Waldeck, and G. R. Fleming, J. Chem. Phys. **78**, 249 (1983).
[43]B. Bagchi, Chem. Phys. Lett. **138**, 315 (1987).
[44]B. Bagchi and G. R. Fleming, J. Phys. Chem. **94**, 9 (1990).
[45]C.-Y. Huang, Z. Getahun, Y. Zhu, J. W. Klemke, W. F. DeGrado, and F. Gai, Proc. Natl. Acad. Sci. U.S.A. **99**, 2788 (2002).
[46]B. S. Kendrick, B. S. Chang, T. Arakawa, B. Peterson, T. W. Randolph, M. C. Manning, and J. F. Carpenter, Proc. Natl. Acad. Sci. U.S.A. **94**, 11917 (1997).
[47]A. M. Tsai, D. A. Neumann, and L. N. Bell, Biophys. J. **79**, 2728 (2000).
[48]J. T. King and K. J. Kubarych, J. Am. Chem. Soc. **134**, 18705 (2012).
[49]R. Walser, A. E. Mark, and W. F. van Gunsteren, Chem. Phys. Lett. **303**, 583 (1999).
[50]S.-M. Park, P. H. Nguyen, and G. Stock, J. Chem. Phys. **131**, 184503 (2009).
[51]I. Lin and M. E. Tuckerman, J. Phys. Chem. B **114**, 15935 (2010).
[52]D. Chandler, *Introduction to Modern Statistical Mechanics* (Oxford University Press, Oxford, 1987).
[53]J.-H. Choi, K.-I. Oh, and M. Cho, J. Chem. Phys. **129**, 174512 (2008).
[54]A. W. Smith, J. Lessing, Z. Ganim, C. S. Peng, A. Tokmakoff, S. Roy, T. L. C. Jansen, and J. Knoester, J. Phys. Chem. B **114**, 10913 (2010).
[55]L. Wang, C. T. Middleton, M. T. Zanni, and J. L. Skinner, J. Phys. Chem. B **115**, 3713 (2011).
[56]M. Kobus, M. Lieder, P. H. Nguyen, and G. Stock, J. Chem. Phys. **135**, 225102 (2011).
[57]S. J. Hagen, Proteins **50**, 1 (2003).
[58]M. Hinczewski, Y. von Hansen, J. Dzubiella, and R. R. Netz, J. Chem. Phys. **132**, 245103 (2010).
[59]J. Sabelko, J. Ervin, and M. Gruebele, Proc. Natl. Acad. Sci. U.S.A. **96**, 6031 (1999).
[60]R. V. Rariy and A. M. Klibanov, Proc. Natl. Acad. Sci. U.S.A. **94**, 13520 (1997).
[61]J. Ma, I. M. Pazos, and F. Gai, Proc. Natl. Acad. Sci. U.S.A. **111**, 8476 (2014).
[62]M. Auton, D. W. Bolen, and J. Rösgen, Proteins **73**, 802 (2008).
[63]S. Shimizu and D. J. Smith, J. Chem. Phys. **121**, 1148 (2004).
[64]S. N. Timasheff, Biochemistry **41**, 13473 (2002).
[65]See supplementary material at http://dx.doi.org/10.1063/1.4897975 for CD spectroscopy, viscosity determination, and a verification of the reproducibility of these experiments.